AIR INFILTRATION REDUCTION IN EXISTING BUILDINGS

4th AIC Conference, September 26-28 1983, Elm, Switzerland

PAPER 9

AIR INFILTRATION IN HIGH-RISE BUILDINGS

CH. ZUERCHER[1] and H. FEUSTEL[2]

[1]Institute of Building Technology
ETH-Z, Hönggerberg
CH-8093 Zurich/Switzerland

[2]Hermann-Rietschel-Institut
TU Berlin
D-1000 Berlin 10/Germany

SYNOPSIS

The prediction of infiltration rates in high-rise buildings caused by superposition of wind pressure across the building skin and stack effect along the building height is a complex problem. For this study, we performed tracer gas measurements and fan pressurization experiments on an eight-storied student residence building in order to determine the influence of wind as well as of the stack effect upon air infiltration. Measured pressure and tracer gas distribution were compared with those from a predictive infiltration computer model for high-rise buildings. To study the influence of the air flow pattern around the building, we adapted the calculated air flow pattern in the stairwell to the measured tracer gas concentration with the aid of various wind velocity profiles characteristic for urban areas and different sets of upwind dependent surface pressure coefficients. This comparison showed, that a satisfactory correlation can only be obtained by application of local pressure coefficients from wind tunnel experiments matching the wind velocity profile as well as the surrounding pattern as close as possible. On the other hand the need for easy to handle examination procedures in building standards asks for more simplified methods.

Keywords

Infiltration, high-rise building, stack and wind effect, leakage area, fan pressurization, tracer gas, wind velocity profiles and surface pressure coefficients, critiical comparison wind tunnel experiments/full-scale measurements

---

Note: an extended version of this report will be published in the Journal "Energy and Buildings"

NOMENCLATURE

c_i	surface pressure coefficient for i-th surface
D	air-permeability: flow coefficient, volumetric air flow rate, at a unit pressure difference for a specified building area ($m^3/Pa^n h$)
in	index: inside
lee	index: leewardside
$\dot{m}$	air mass flow (kg/h)
n	pressure exponent, between 0.5 and 1
NPL	neutral pressure level
out	index: outside
p	pressure (Pa)
$\dot{Q}$	volumetric air flow (m^3/h)
v	wind speed (m/s)
wind	index: wind or -wardside
z	z-coordinate or height of the building (m)
α	exponent in the power-law for the vertical wind velocity profile, depending on terrain roughness
Δ	difference in conjugated item
ρ	density (kg/m^3)
θ	temperature (^oC)

1. INTRODUCTION

To predict possible condensation zones and to optimize the energy conservation in buildings, the measurement and control of air movement through a building structure has become more and more important. But probably one of the deficiencies in most computerised methods to predict energy requirements of buildings is the lack of reliable algorithms to model air infiltration sufficient precisely. In contrast to the relatively steady process of heat transmission, infiltration is more strongly influenced by rapid changes in weather conditions. Moreover, infiltration is nonlinear, depending primarily on wind pressure and thermal buoyancy (stack-effect), and therefore difficult to model.

Infiltration is an important component of the space-conditioning load, especially in houses with above average shell thermal performance. As houses are made tighter to reduce infiltration losses, the maintenance of acceptable indoor air quality begins to be an issue of concern[1]. Balancing the competing demands of energy conservation and air quality may require a target ventilation rate for a structure. This, in turn, demands the existence of inexpensive instrumentation to measure infiltration or a model that will accurately predict air movement in buildings[2].

Infiltration, the random flow of air through openings in the building surface, is for a single-family house largely independent of the house type and structure. This flow process is dominated by the leakage structure of the building rather than by structural type. Air flow is the consequence of pressure difference due to wind pressure and thermal buoyancy. Besides these driving forces, the infiltration rate, however, depends on the air-permeability of the building structure and on the distribution of leakage areas throughout the building.

A prediction of the infiltration for high-rise buildings is a more complex problem. The pressures that drive the flow are the result of the superposition of wind pressure that depends on the elevation and orientation and the stack-effect. Recent works on prediction models for one-family houses[3,4] demonstrate the strong influence of the stack-effect on the infiltration rate. The latter is even more important for high-rise buildings because of the magnitude of the building height[5].

2. AIR INFILTRATION DUE TO STACK- AND WIND EFFECT

Air flow through a building shell is a combination of laminar and turbulent flow through openings and cracks. The former is proportional to the pressure difference over the envelope whereas the latter varies with the square root of the pressure difference.

Two differenct driving mechanisms are primarily responsible for natural air flow in buildings -- wind pressures and buoyancy forces. Compared to the static pressure in the undisturbed wind velocity pattern, the pressure field around a building is characterized roughly by regions of overpressure on the windward façade and underpressure on façades parallel to the air stream or on the leeward side of the building respectively.

$$p_{wind} = 1/2\ \rho(z,T)\ v^2(z)\ c_i(z)$$

The c_i-values ("shielding coefficients") can be determined either from measurements on full-scale buildings or on corresponding small-scale models in a boundary-layer wind tunnel[6,7].

Excluding thermal stratification, the vertical profile of the mean wind speed in the atmospheric boundary layer depends primarily on the surface roughness and shows an increasing velocity with height above ground, approximated by a power-law expression[8].

$$v(z) / v(z_0) = (z/z_0)^{1/\alpha} .$$

Usually, $v(z_0)$ is a meteorological reference wind speed recorded at a standard height of z_0 = 10 m above ground.

Pressure gradients between inside and outside of the building also arise from changes in air density due to temperature differences between ambient air and air inside (stack-effect)

$$\Delta p_{stack} = g\ (\rho_{out} - \rho_{in})\ (z - z_{NPL}) ,$$

with z_{NPL} as the neutral pressure level, the height on the building façade where the interior pressure equals the exterior. The stack-effect pressure gradient only depends on the absolute inside/outside temperature, whereas the height of the NPL will be determined by the air leakage distribution. In practice the NPL height is rarely knwon and stack pressure is normally expressed relative to the lowest opening.

Referring to infiltration, a building can roughly be described with the aid of the four following border-line cases[5]:

a) row house
b) detached house

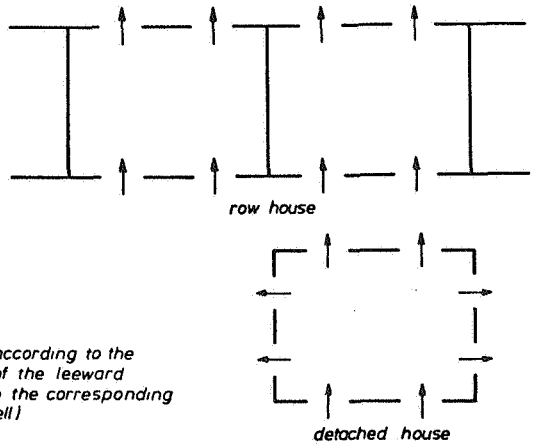

Fig. 1a:

Subdivision of the building type according to the permeability ratio (leakage area of the leeward windows and doors compared to the corresponding value over the total building shell)

c) story-type construction
d) shaft-type construction

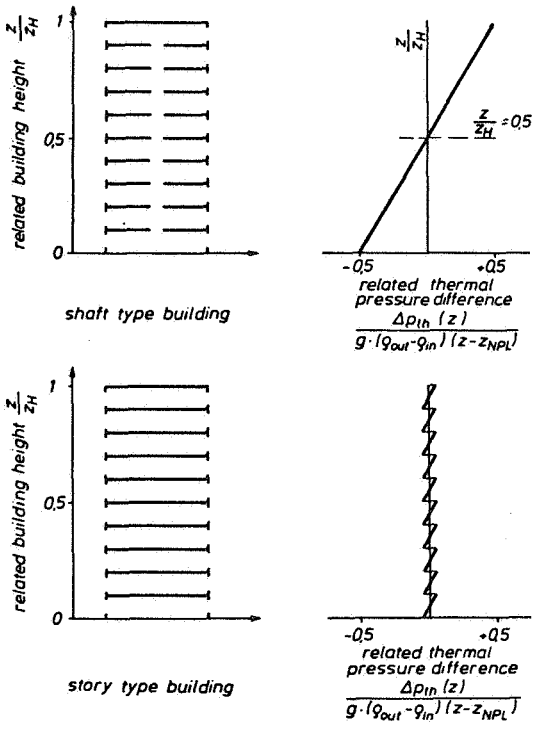

Fig. 1b:

Thermal pressure difference as a function of the type of construction for $t_{in} > t_{out}$ and the air leakage uniformly distributed over the building shell

This subdivision into four basic categories is based on a comparison of the permeability behavior of a building as function of its location (influence of wind effect) as well as of its construction type (influence of stack-effect).

The influence of wind flow on the building with overpressure on the upwind and underpressure on the separated walls will be determined by the permeability ratio R (= total permeability walls separated from wind flow / overall permeability building façades). Row houses can be described with an average R-ratio of 0.5, whereas the corresponding value for detached houses rises up to 0.7.

In a shaft-type building the buoyancy forces will grow up extremely strong contrary to the story-type counterpart with its small stack effect only within each story.

3. EXPERIMENTS

3.1 Test building - location and layout

The four dormitories comprising Unit I of student housing for the University of California at Berkeley occupy a 0.9 ha site two blocks south of the campus. The surrounding blocks are mostly three-story residential apartments. The dorms are identical nine-story buildings, arranged on the periphery of the block, oriented both north/south and east/west. The structure is reinforced concrete with metal curtain walls and cast stone grills on the exterior wall of the utility rooms.

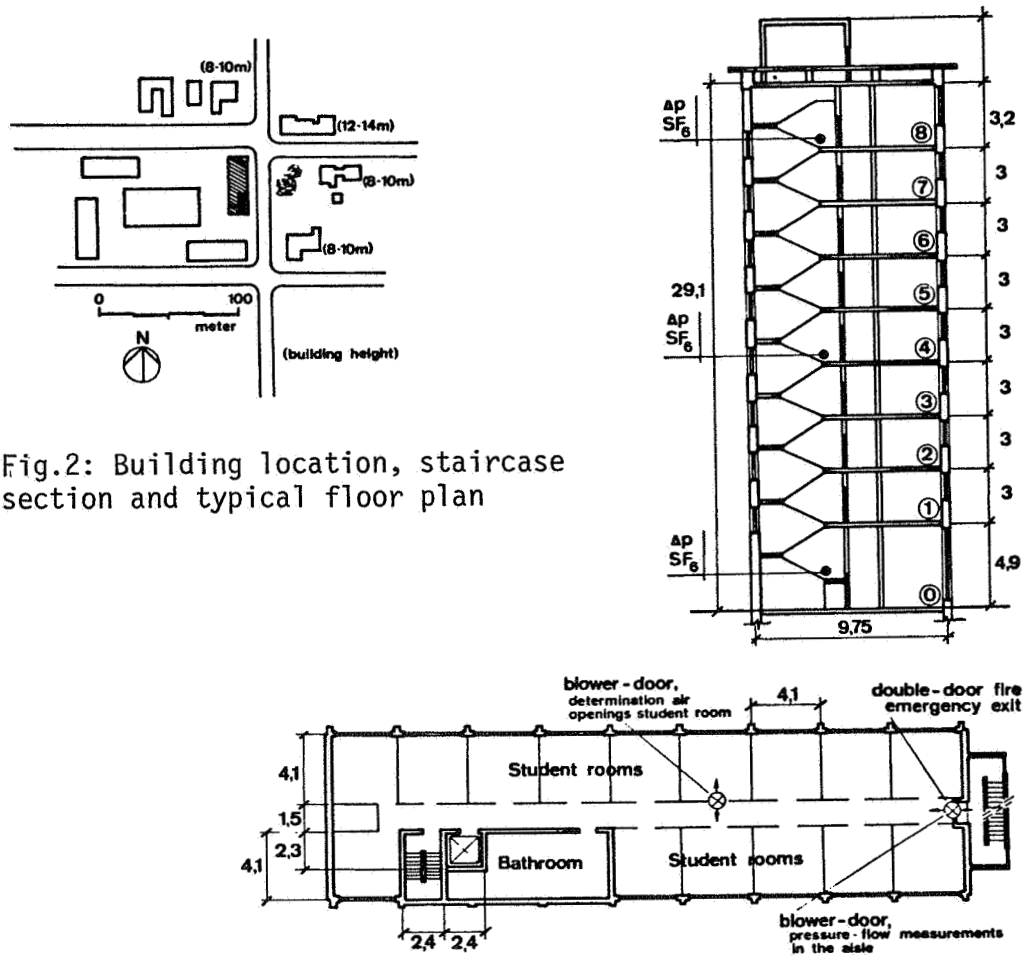

Fig.2: Building location, staircase section and typical floor plan

3.2 Blower-door measurements

The pressure-flow characteristics for specific building parts were measured using a door-mounted, variable-speed fan capable of moving large volumes of air into or out of a structure. Natural infiltration is typically driven by pressure differences across the building shell in the range of 0 Pa to 10 Pa and is characterized by large, short-term fluctuations. When Δp is larger than 10 Pa, fan flow dominates natural infiltration and the latter may be disregarded. At a given Δp and a fan speed, the flow of air is determined indirectly by means of a previously established calibration curve (i.e. from flow vs. RPM characteristics at different pressure differences). With the aid of measurements at discreet Δp's in the over- as well as underpressure region (-70 Pa to +70 Pa), the parameters D and n are fitted to the following equation characterizing the air flow through a leaky building shell:

$$\dot{Q}(\Delta p) = \dot{Q}_{fan}(RPM, \Delta p) = D\ (\Delta p)^n\ .$$

As example the following graph demonstrates the different pressure-flow regimes in the stairwell due to changes in leakage area by opening previously sealed air cracks.

Boundary-conditions	Press		Depress	
	D ($m^3/Pa^n h$)	n -	D ($m^3/Pa^n h$)	n -
-all doors sealed	262	0.52	241	0.63
-emergency exit unsealed	362	0.47	264	0.61
-emerg. exit and roof door unseal.	345	0.49	323	0.61
-all doors unsealed	690	0.47	456	0.62

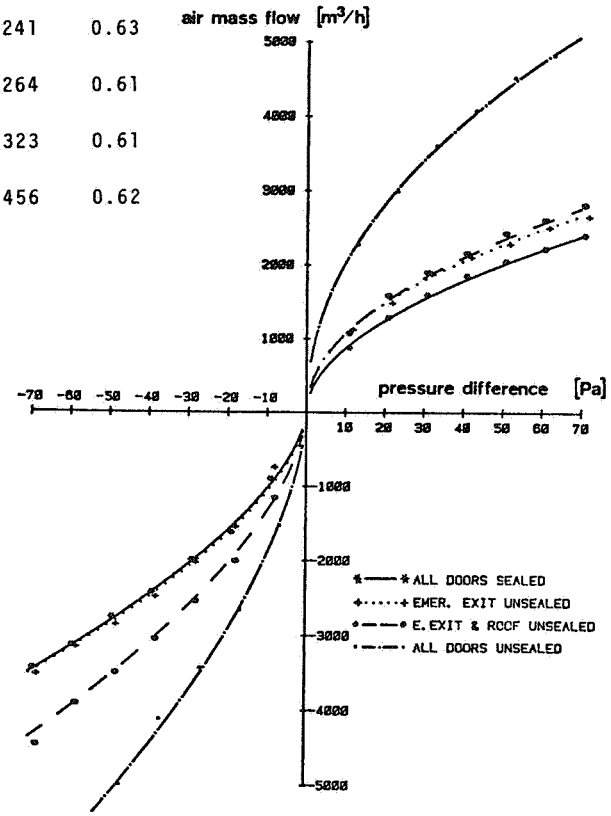

Fig.3: Pressure-flow characteristics and air leakage parameters for different structure parts of the stairwell (blower-door measurements)

3.3 Tracer gas and pressure measurements

The air flow in the stairwell was determined using a tracer gas technique. Injecting SF_6 at the ground-floor at an electronically controlled constant flow rate, its concentration at the 1st, 4th and 8th floor were recorded together with pressure differences (ground-floor and 8th floor) and temperatures as a function of time. Multiple sampling throughout the stairwell crossections provided properly averaged measurements of the SF_6 concentrations at the selected floor levels.

The tracer gas concentration itself was determined from infrared transmission losses in an 1.5 m gas cell.

A capacitive potentiometer with a thin, prestressed metal diaphragm as variable, sensitive element was used as differential pressure sensing element.

4. COMPUTER SIMULATIONS

The calculation of natural ventilation rates in a building is a

complex task. Simulation programs using an iteration method are normally based on a network containing a large number of non-linear equations. Therefore, the only useful tool to get a solution is a digital computer[9].

A routine, developed at the Hermann-Rietschel-Institute[10,11] and which was the framework for the computer model used in this study, calculates solutions of its non-linear equations system using Newton's iterative method. The building to be examined will be subdivided in zones with the aid of a threedimensional scanning field. The grid elements are represented by nodes each associated with a zone pressure. These nodes are connected among themselves via the zone boundaries characterized by their permeabilities, exponents of the pressure difference and mass flows. With floors, stairwell and elevator shaft represented by a series of rooms (nodes), each at a specific pressure and temperature, the movement of air through the building will be computed by a program based on steady-state pressure dependent mass flow balances at each floor as well as in the two shafts (elevator shaft and stairwell). The net mass flow between in- and outgoing air through the air openings of the r-th surface will be calculated by:

$$\dot{m}_r = \rho \, D_r \, (\Delta p)^{n_r}$$

with experimental permeabilities D_r and pressure exponents n_r from blower-door measurements.

In a first run, the wind-induced pressure field around the building was calculated using an exponential wind velocity profile for urban areas ($\alpha \sim 3$[12]) and mean pressure shielding coefficients of 1 for the upwind and -0.3 for separated flow regions (sides, rear, flat roof). According to meteorological data from the measuring period the mean wind direction for calculations was selected to be from east. For such wind directions perpendicular to a main building façade, the wind pressure at a specified height will normally be idealized by width-undependent pressure coefficients for each surface orientation. Therefore, at each floor, all rooms with equal door- and window permeabilities and the same orientation as for the façade, can be mathematically treated as one room. Since permeabilities are additive like conductances in an electrical network, such a simplified room can be attached to a resulting permeability. Hence, the flow resistance for a window and a door located in series as e.g. in the student rooms will be calculated to

$$R = D_{tot}^{-1} = (D_{window}^{-1/n} + D_{door}^{-1/n})^{n}$$

In the building to be investigated, a storey containing all student rooms, lounge/loundry and aisle, except the corresponding portions of the stairwell and elevator shaft, can be described by substitute resistances related to each façade. The stack-effect pressure gradient was calculated on the basis of temperature in-

duced air density differences.

The following figures will outline principal results obtained from the calculations of the air flows in the building and the pressure gradients in the construction as a function of different weather conditions. Considering the net ingoing air flow for the entire building without referring to any special building surface, at 0 m/s wind speed and an averaged ambient air temperature of 13°C, there will be no infiltration loss in the building due to ventilation except for stories lower than the 6th floor.

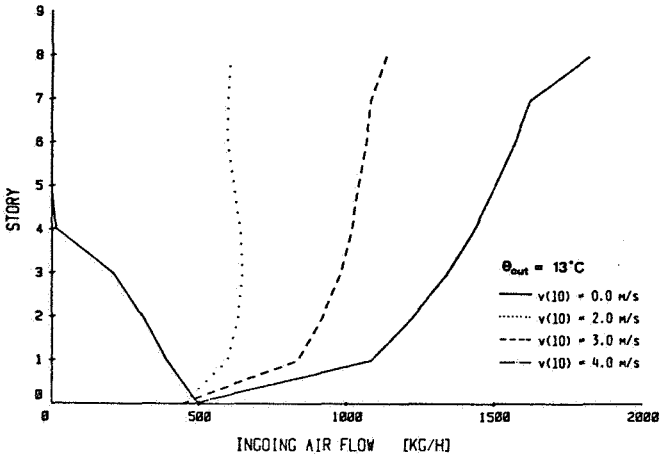

Fig.4: Influence of wind velocity on air flowing into the building (θ_{out} = 13°C)

With increasing wind speed the shape of the ingoing air flow curve will be more and more influenced by its power-law velocity profile. It is remarkable that the air flow at the ground-floor will not be influenced by changes in wind speed. In the elevator shaft -- independent from wind speed -- air from floors below the 5th level flows to the shaft, whereas the emanation of air from higher levels increases to its maximum at the 8th floor. Therefore, as a consequence of conservation of mass, an air current in the elevator shaft will transport groundfloor-air to higher levels. Such an air exchange in the building may have undesired accompaniments such as the transport of air pollutants[13] or of odors in apartment houses. Moreover, for the safety of occupants, such studies are a helpful tool to estimate the smoke movement in a building during a supposed fire.

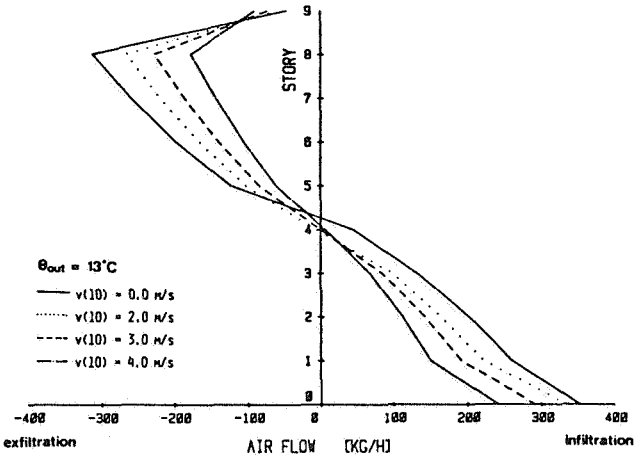

Fig.5: Air flow through openings of elevator shaft for different wind speeds (θ_{out} = 13°C)

On the other side, the air flow in the staircase demonstrate a quite different behavior. To study this flow regime, we plotted the calculated data for both the air flow from the staircase

through the windward (outside) wall air openings and the air current staircase-adjoining floors. The flow regime in this part of the building is governed on one side by air flowing into the structure at lower levels and on the other side, with increasing wind speed, by a decreasing air loss at higher levels. The neutral air flow level rises up with increasing wind velocity. Higher wind forces at the façade due to wind speeds larger than about 3 m/s will press ambient air into the staircase, even at the top of the building. This additional air flow increases the inside pressure to such a degree that the ground-floor staircase pressure will even exceed the outside pressure at this height, leading to an outflow of air.

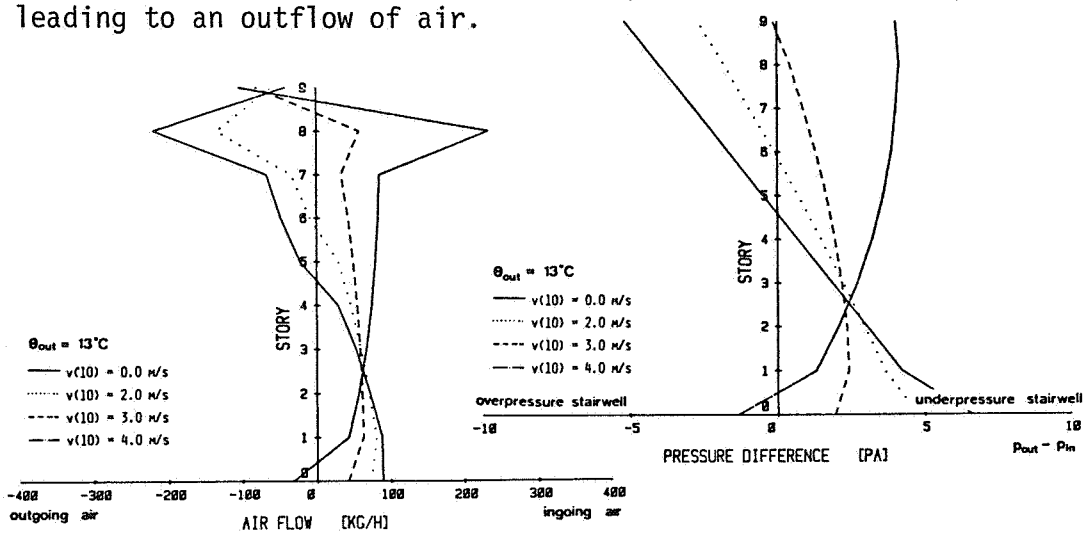

Fig.6 and 7: Computer calculated in-/exfiltration flows in the staircase through air leakages in the outside windward surface of the building (left) and their driving pressure difference forces $\Delta p = p_{out} - p_{in}$ (right) as function of the building height ($\theta_{out} = 13^{o}C$)

Higher wind speeds cause air flows from the shaft into the corridors through all staircase doors, whereas at wind speeds smaller than 2 m/s indoor air from the student rooms and the corridors is pressed into the shaft only at lower levels. There will be no air exchange between the different floors through the staircase.

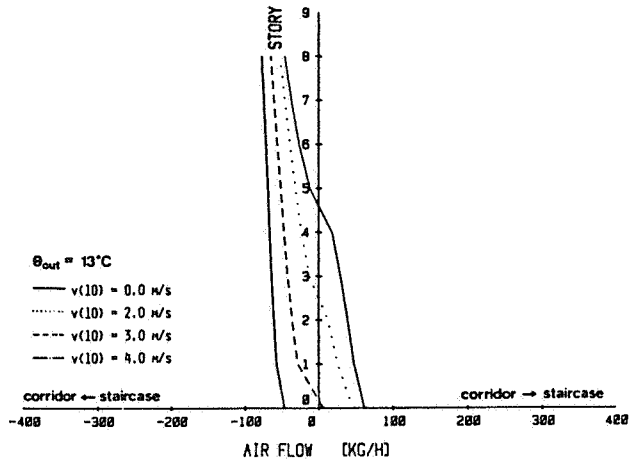

Fig.8: Wind effect onto the air current from the corridors to the staircase at different floor levels ($\theta_{out} = 13^{o}C$)

The temperature dependence of the net air flow throughout the whole structure demonstrates a well known phenomena for low tem-

peratures. Especially in areas characterized by low winter temperatures, the overall energy demand for a heating period to equal the ventilation heat load at the ground-floor due to natural ventilation will be at least a few times higher than the equivalent amount needed to heat the top floor[14]. In our building, at a supposed outdoor temperature of $\theta = -15^{o}C$, the above-mentioned ratio would rise up to 5.5. On the other hand smaller temperature differences lead to a more balanced air current as a function of building height.

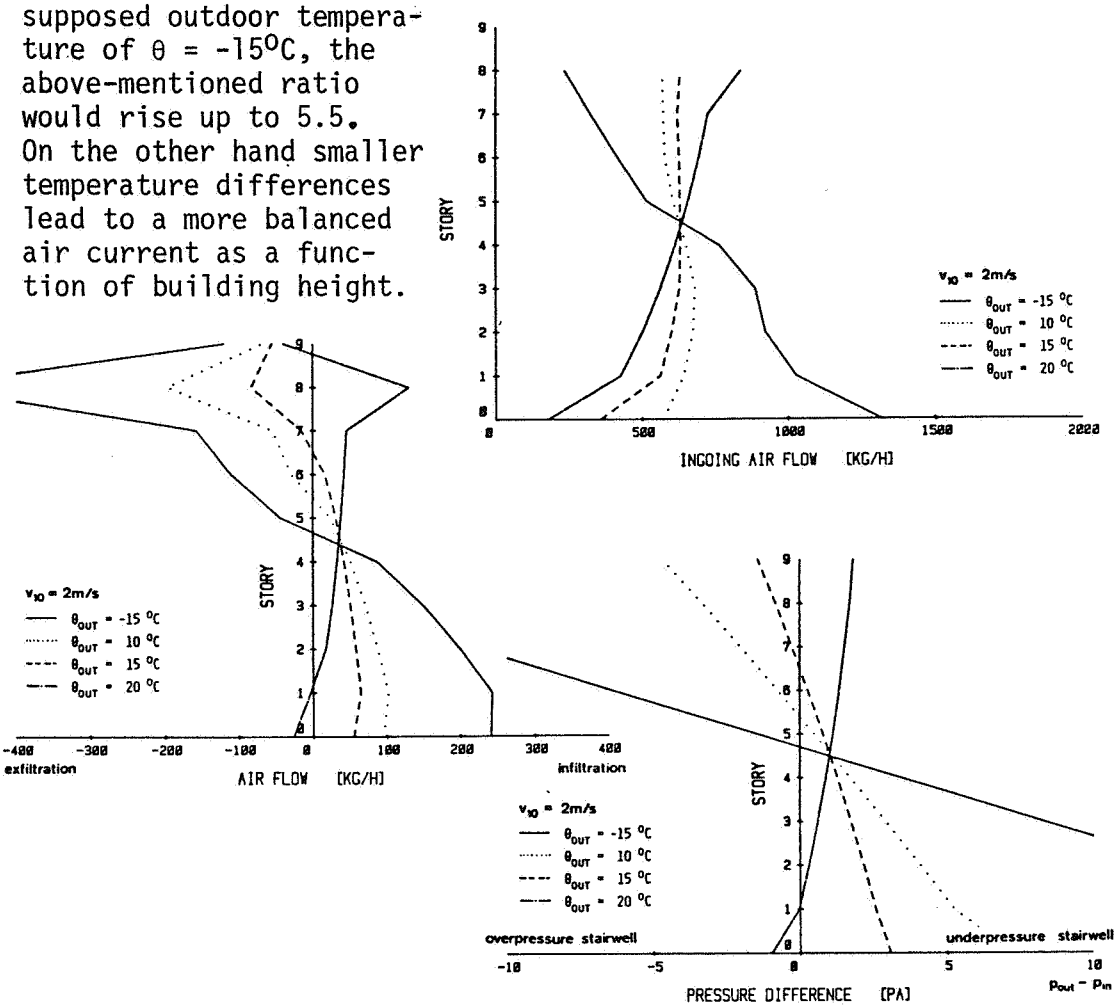

Fig.9/10/11: Temperature- and height dependence of
- total air flow into the building (top)
- air flow through openings in the outside surface of the staircase (middle)
- pressure differences between windward building façade and staircase (bottom)

This calculation example clearly shows, that space conditioning due to natural ventilation losses calls for a very sensitive control of the room heating system.

5. COMPARISON - MODEL AND MEASUREMENTS

5.1 Wind and surface pressure coefficients

Since there exists no mathematical expression to calculate accurately the air flow pattern around a building, the latter is still difficult to predict and changes for the same building shape from location to location due to the influence of nearby structures. Especially the flow pattern in front of the windward façade will be strongly affected by upstream structures. This streamline pattern striking the front of a tall building will be divided in an upwind flow at higher levels and a lower region governed by downstreaming wind, both separated by a stagnation zone. The second one separates from the building façade before reaching the ground level, creating a standing vortex near ground with sometimes high internal wind velocities. Therefore, especially near ground level, the wind pressure pattern has to be examined very carefully.

Before discussing the tracer gas measurements we outline the difficulties using height independent surface pressure coefficients. A first comparison showed that e.g. the pressure differences measured at the ground- and 8th floor level cannot be explained by our previous and rough calculations.

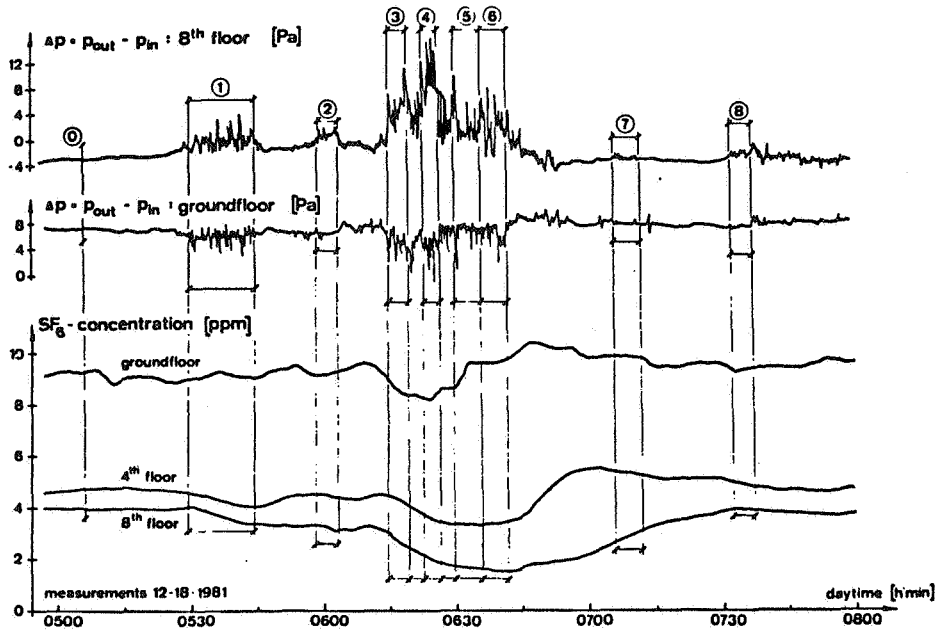

Fig.12: Extract from pressure- and tracer gas measurements at the dormitories, average outside temperature $\theta_{out} = (12 \pm 1)^{o}C$

Based on this outcome, in a first step, an arbitrary modification of the wind velocity profile taking into account higher wind pressures near the ground (0 m < z < 10 m) led to a much better agreement but was still not satisfactory. Calculations with ave-

raged pressure coefficients from Akins et al.[15] and ASHRAE Fundamentals[16] based on a reference wind velocity measured at the roof level as well as height dependent surface coefficients from Jackman and Tech[17] even led to increasing pressure differences $\Delta p = (p_{out} - p_{in})$ for both levels - groundfloor as well as 8th floor - with increasing wind velocities.

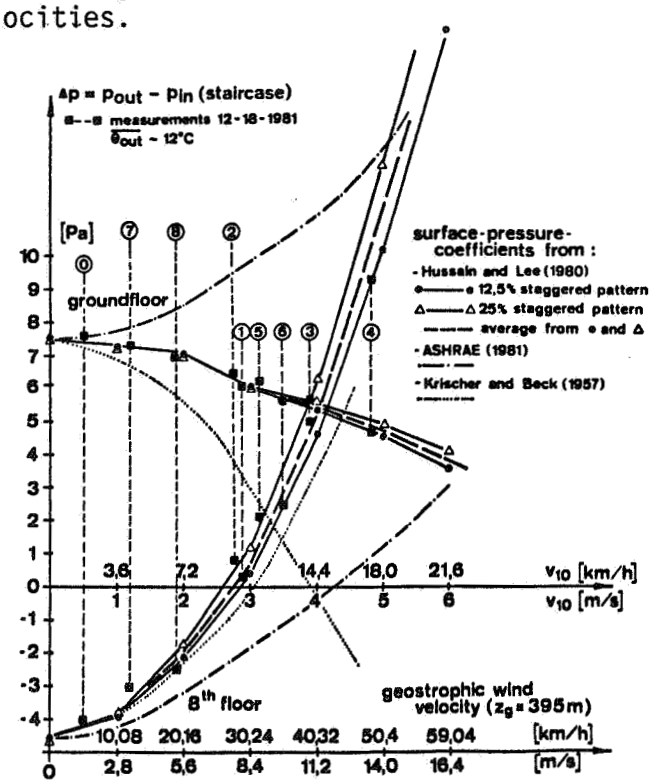

Fig.13: Comparison of the calculated pressure differences at the ground- and 8th floor for different surface pressure profiles.

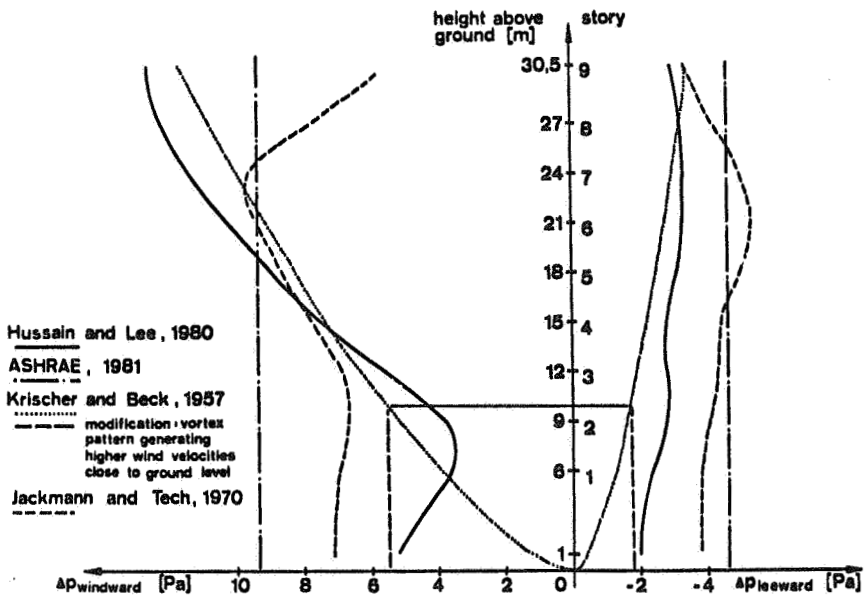

Fig.14: Comparison of the different wind pressure profiles tested in this computer simulation study (v_{wind} (10 m) = 3 m/s)

Only a critical analysis of the built environment and the application of boundary-layer wind tunnel results from Hussain and Lee[6] yielded satisfactory results over the whole observed wind speed range. These authors have studied the surface pressure profiles on a high building as function of different upwind patterns and various height ratios (central building height to average height of the surrounding structures). Since there exists no experimental values for a staggered pattern of about 18%, corresponding to the upwind built-up area in front of the student residence building, we took average values from 12,5% and 25% staggered pattern experiments at a height ratio of 3. In such a way it was possible to correlate pairs of measured pressure differences in the wind velocity range of 0 km/h to 18 km/h at 10 m above ground.

This study clearly demonstrates the discrepancy between the overhasty application of simplified and constant surface pressure coefficients in combination with an exponential equation for the wind velocity profile. Representative average surface pressures - even combined with a questionable correction for the lower wind velocities near ground level[16] - seem not to be the right tool to calculate air in-/exfiltrations, especially for high-rise buildings with near ground vorticity effects and/or large roof overhangs.

5.2 Tracer gas measurements

Fitting the tracer gas equation to the measured SF_6 concentration curve with the aid of an inductance variation, we can extrapolate for calm weather conditions an air exchange rate at the ground-floor of the staircase of 3,5 h^{-1} and an effective space volume of about 75 m^3. The latter is about two times larger than the expected physical volume of space at the injection place. This discrepancy can be explained either by the attached stairwell space communicating with the injection anteroom or by a non-recognized significant nearby air leakage participating in the air exchange and thus increasing the effective volume. On the other side, together with an approximated physical space volume of 30 m^3 for the two anterooms of the stairwell (entrance from the lobby and through the rearward ground-floor emergency door), we estimate an air flow of 105 m^3/h from the ground floor to the first floor. This estimation agrees well with the computed value (table I). Regarding the mixing time the ground floor SF_6 concentration calculated by the fitted tracer gas equation reaches after 50 min 95% of the equilibrium concentration. The parameter matching for the time behavior of the SF_6 concentration at the 4th and 8th story shows a time delay of the "theoretical" onset of the gas mixing of about 20 min and 45 min respectively.

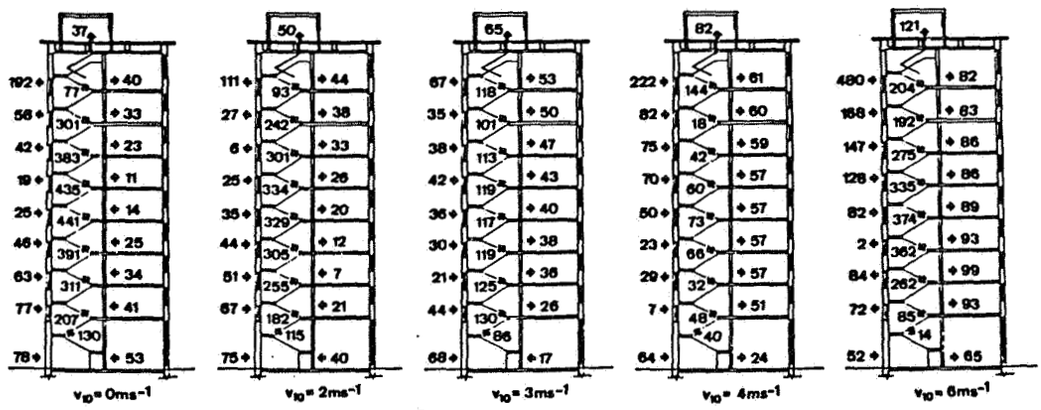

Table I: Air mass flow (m^3/h) throughout the stairwell for wind speeds v_{10} of up to 6 m/s, $\overline{\theta_{out}} \sim 12^{o}C$

The tracer gas measurements (figure 12) prove the following behavior: With increasing wind speed, the SF_6 concentration at the ground-floor shows a slowly increasing trend up to a wind speed of 4 m/s to 5 m/s where the gas content decreases due to outside air which is pressed down through the staircase. Also at the 4th and 8th level we observe the same behavior but already at lower wind speeds because the flow regime at higher levels is much more influenced due to higher wind pressures on the building. A summary of the calculated air mass flow in table I clearly demonstrates how the flow regime, dominated by the stack effect at low speeds, changes over to a reversed situation, where, principally due to wind effect a lot of air is pressed into the building through the windward air leakages at the upper levels and pours out at lower stories. At a wind speed of about 3 m/s a homogenous intermediate state is built up where air is pressed into the building along the whole windward façade and no air flow downwards the staircase can be observed. For wind speeds v_{10} lower than 3 m/s only small changes in the tracer gas concentration at the different test levels were observed (figure 12, period 0, 1, 2, 7 and 8). The latter values are according to order in agreement to the SF_6 content estimated from the computed air mass flows. Referring to table I the flow regime at the 4th floor changes from up-to downwards at wind blowing with 3 m/s to 4 m/s (compare e.g. end of period 1 in figure 12). With increasing wind pressure matching the measuring periods 3 and 4, all gas concentrations show a decreasing trend, also the ground-floor value. This is due to the change in the air flow direction in the stairwell between story 0 and 1 in the wind speed range of 4 m/s to 6 m/s. With less wind in the following observation intervals, the SF_6 concentration at the injection place starts to increase whereas the adequate values in agreement with the flow situation represented in table I still slowly decrease. Meanwhile the ground-floor SF_6 level shows an increasing trend, the tracer gas content for the 4th level stays nearly constant due to the change in the direction of flow around 3 m/s to 4 m/s, but still decreases at the 8th floor because at every floor air containing SF_6 is lost into the aisles (period 5 and 6). The last regime only changes when the wind pressure collapses and the buoyancy behavior for low wind speeds starts to be dominant in the staircase.

6. CONCLUSIONS

To predict energy saving infiltration reductions with the aid of air flow calculations it is necessary to know the actual pressure distribution along the building façades. This can only be done by using local pressure coefficients from wind tunnel experiments matching the wind velocity profile as well as the surrounding building pattern as close as possible.

The characteristics of natural wind are well understood, but the local influences of surrounding topography are difficult to predict. Coefficients based on wind tunnel experiments performed on simple building shapes are widely available but may not be applicable to buildings shielded by local obstructions. Much work is still required to develop simple rules to cope with this problem.

On the other hand the need for easy to handle examination procedures in building standards asks for more simplified calculation methods, e.g. the application of constant surface pressure coefficients combined with a wind velocity profile modified at lower levels and the edges of the roof taking into account the environmental pattern and the upwind landscape structure.

In the future, more research will also be needed in
- transport mechanisms in the building (e.g. air movement room to room with large openings; convective air flow)
- air infiltration in rooms of the same building but with different heights and orientations.

REFERENCES

1. Wanner, H.U.: Indoor air quality and minimum ventilation, 2nd Air Infiltration Centre (AIC) Conference: Building Design for Minimum Air Infiltration, Stockholm (1981)
2. Carnahan, W. et al.: Efficient Use of Energy, AIP Conference Proc. 25, part III, section C6, 81 (1975)
3. Sherman, M.: Air infiltration in buildings, Ph.D. Thesis, Lawrence Berkeley Laboratory (LBL), LBL-10712, Berkeley (1980)
4. Alexander, D.K. and Etheridge D.W.: The British Gas Multicell Model for Calculating Ventilation, ASHRAE Trans. 86(II),(1980)
5. Esdorn, H. and Brinkmann, W.: Der Lüftungswärmebedarf von Gebäuden unter Wind- und Auftriebseinflüssen, Gesundheits-Ingenieur 99(4), 81 (1978)
6. Hussain, M. et Lee, B.E.: An investigation of wind forces on three dimensional roughness elements in a simulated atmospheric boundary layer, Dep.Build.Sci. reports BS 55-57, University of Sheffield (1980)

7. Dagliesh, W.A.: Comparison of model/full-scale wind pressures on a high-rise building, J. Ind. Aerodynamics 1, 55 (1975)

8. Cermak, J.E.: Aerodynamics of Buildings, Ann. Rev. Fluid Mechanics 8, 75 (1976)
Davenport, A.G.: The interaction of wind and structures in "Engineering Meteorology", Elsevier, Amsterdam, 527 (1982)

9. Feustel, H.: Research into the Ventilation of Dwellings - Theory before Practice, AIC - Translation No. 14

10. Esdorn, H. et al.: Bauliche und lüftungstechnische Massnahmen gegen unerwünschten Luftaustausch zwischen Räumen unterschiedlichen hygienischen Standards, Final Report of the TP F2/2 of SFB 159, TU Berlin (1976)

11. Feustel, H. and Esdorn H.: Mass flow distribution in high-rise buildings with forced ventilation systems, Proc.Int.Conf. System Simulation in Buildings, Liège, Belgium (1982)

12. Davenport, A.G.: A rational for the determination of basic design wind velocities, J. Struct. Div. 86, 39 (1967)

13. Feustel, H.: Schutzdruckhaltung - ein Mittel zur Reduktion des aerogenen Keimtransportes, Proc. 5th Symp. on hospitals, Hannover (1978)

14. Esdorn, H. and Feustel, H.: Maschinelle und freie Lüftung von Wohngebäuden - ein Vergleich, Proc. XXI Int. Cong. Building Services Engineering, Berlin (1980)

15. Akins, R.E. et al.: Averaged pressure coefficients for rectangular buildings, Proc. 5th Int. Conf. Wind Engineering, Fort Collins, Colorado, Vol. 1, 369 (1979)

16. - Air Flow around buildings, ASHRAE Handbook of Fundamentals, chap. 14 (1981)

17. Jackman, P.J. and Tech, B.: A study of the Natural Ventilation of Tall Office Buildings, J. of Int. Heating and Ventilation Engineer 38, 103 (1970)